Manuscipt of the book chapter: Indium an efficient co-catalyst in novel Cu or Ni catalysts for selective reduction of biomass derived fatty acids to alcohols,
in Indium: Properties, Technological Applications and Health Issues
Editors: Hsaio G. Woo, Huang Tsai Choi
Nova Publishers, New York, 2013, P 53-81.
ISBN: 978-1-62257-696-8

Indium an efficient co-catalyst in novel Cu or Ni catalysts for selective reduction of biomass derived fatty acids to alcohols

György Onyestyák, Szabolcs Harnos, and Dénes Kalló
Institute of Materials and Environmental Chemistry, Research Centre for Natural Sciences, Hungarian Academy of Sciences, Budapest, Hungary

ABSTRACT

Supported copper or especially nickel catalysts are very important for hydrogenation of various organic compounds in the practice. Activity, selectivity and stability can be greatly improved using co-catalysts: e.g. chromium compounds with Cu (Adkins catalyst for fatty alcohol production) or molybdenum compounds with Ni (for hydrodesulfurization [HDS], hydrodeoxygenation [HDO], hydrodenitrogenation [HDN], etc. catalysts in petroleum refining.

Recently, we discovered novel highly efficient bimetallic supported catalysts which were exceedingly active and selective in the hydrodeoxygenation (HDO) of octanoic acid to octanol at moderate pressure and temperature in addition very effective in reduction of acetic

acid to ethanol. The catalysts contained indium as co-catalyst and a metal of high hydrogenation activity, such as, copper or nickel, on various support. A significant synergism can be observed when indium with another metal of hydrogenation activity is applied. Appearance of Cu_2In or Ni_2In phases, intermetallic compounds on the surface of metal particles results in significant increase of desired hydrogenation activity, i.e., in stepwise hydrogenation of carboxylic acids stopped at alcohol formation and in inhibiting hydrogenations when hydrodecarbonylation of carboxylic acids (loss of one carbon atom) and hydrogenolysis of hydrocarbon products (loss of further carbon atoms) proceed. Moreover, in presence of mobile indium atoms or of indium containing nano clusters mono- or bimolecular alcohol dehydration capability of the support is selectively poisoned.

In order to have more information about the role of indium, experiments are carried out using quite different hydrogenation metals, Cu and Ni. Hydrogenation experiments are carried out with long chain fatty acid like octanoic acid for production of octyl alcohol and short chain acetic acid (produced in large amounts from biomass) for production of ethyl alcohol, ethyl acetate or acetaldehyde. The main question is how the co-catalyst second metal of moderate hydrogenation activity as gallium, cadmium, tin, but first of all indium, modify the activity of the supported hydrogenation metal and the surface properties of the support.

1. INTRODUCTION

Addition of a second component to metal catalysts is widely used in order to enhance activity and/or selectivity. The removal of heteroatoms (S, N, O) from petroleum fractions is one basic step in refining to produce transportation fuels and chemicals of desired quality. Using petroleum fractions the heteroatoms should be removed at a low concentration level of contaminating compounds. Nowadays, biomass materials coming to the front as renewable

resources contain oxygen in very high concentration. So, novel, more efficient catalysts are needed.

Fatty alcohol is one of the first chemicals of natural origin (produced from fatty acid content of fats or vegetable oils) and used in high volume. In 1931, Adkins suggested to use copper chromite catalysts for selective hydrogenation of fatty acid methyl esters to fatty alcohols [1]. The use of chromium is limited by its toxicity. There are worldwide efforts to find alternative catalyst systems.

The major industrial use of supported metal sulfides is the removal of sulfur, nitrogen, oxygen and metals from the most hydrocarbon streams in refineries by reduction in hydrotreating processes. Hence this is the catalytic technology comprising the largest material processing per year. Hydrotreating catalysts contain molybdenum and cobalt or nickel, supported on γ-Al_2O_3. Molybdenum sulfide is traditionally considered as the catalyst and Co or Ni is considered to promote the Mo activity [2]. Removal of oxygen from oxygen-containing molecules was especially important for the treatment of coal-derived liquids. Biomass-derived feedstocks have been recently introduced into refineries posing new challenges for refining processes and catalysis. Due to high oxygen content of biomass feedstocks, deoxygenation processes play an important role in upgrading of these raw materials. The economics seems to be favorable for conversion of edible biomass (vegetable oils) to fuel containing carboxyl groups only which can be efficiently converted. Investigations of conventional sulfided HDS catalysts, such as CoMo, NiMo, NiW supported on alumina, have revealed that complete conversion of triglycerides to hydrocarbons can be attained over these contacts [3]. The studies have shown that two reaction pathways, i.e. hydrodeoxygenation and hydrodecarboxylation, are responsible for hydrocarbon formation. The extent of these different reaction routes depends on the catalyst choice and reaction conditions [4, 5].

When HDS catalysts are applied addition of sulfur containing compounds into the reaction zone is required to maintain the catalyst activity. If non-sulfided catalysts are used the inconvenient sulfurization step can be omitted. Thus, the goal of this work is to develop non-sulfided catalysts for upgraded bio-fuel production.

Recently, we discovered novel highly efficient bimetallic alumina supported catalysts which are highly active in the selective reduction of octanoic acid to octanol [6]. The catalysts contained zerovalent indium as co-catalyst and a metal of hydrogenation activity, such as copper or nickel.

Indium is a rare post transition metal, the 61st most abundant element of the Earth core, however, plays important role in various applications. Consequently, its price is high and increases with the increasing demands. In the middle of 1980s, the development of indium phosphide semiconductors and indium tin oxide films for liquid crystal displays (LCD) aroused much interest. By 1992, the thin film application had become the largest end use. Catalytic applications appeared in various forms nowadays, but this role seems to be rather promising.

A number of studies showed that In-zeolites have significant activity in the selective catalytic reduction of NO to N_2 with light hydrocarbons in the presence of excess oxygen (NO-SCR) [7], which reaction has great practical importance especially in the abatement of NO_x emission of boilers and engines fuelled by natural gas. Alumina supported In_2O_3 catalyst demonstrates also good NO_x reduction performance [8]. Supported In_2O_3 catalyst was proven to be a novel efficient catalyst for dehydrogenation of propane with CO_2 [9] or N_2O [10]. Pure In_2O_3 was revealed to act as a surprisingly efficient and promising, highly active and selective catalyst for steam reforming of methanol to $CO_2 + H_2$ [11]. Although, increasing attention has lately been paid to indium containing catalysts for methanol steam reforming, first Y Men

et.al. assumed that using alumina supported Pd in intimate contact with In_2O_3, the active phase presumably is in form of a PdIn alloy [12].

In the trimetallic SnInPt/alumina gasoline-reforming catalyst In is present in zerovalent unalloyed form or in Pt_xIn alloys not changing the electronic properties of Pt [13]. Indium was not found to be a good promoter instead of copper for the Fe-based Fischer-Tropsch synthesis (FTS) catalyst because of the melting of indium during the FTS reaction [14]. Platinum catalysts supported on corundum promoted by indium and tin were successfully applied for the selective dehydrogenation to propylene [15]. Although the catalysts were reduced in hydrogen flow at 500 °C in situ the reactor, surprisingly the structure of the bimetallic active components on corundum could be described as relatively highly dispersed metal-ionic system. Tin and indium addition to $MgAl_2O_4$ supported Pt catalyst lead to an excellent performance in the butane dehydrogenation reaction [16].

Nowadays, bimetallic In containing catalysts are coming to the front in reductions, too. Technologies for removal of nitrate from drinking water and waste water will be required in the near future, and catalytic nitrate reduction is one of the most promising methods. So far, the understanding of nitrate reducing catalysts has been very poor. InPt/alumina catalysts were characterized by EXAFS and XANES [17]. The results confirm that for the nitrate hydrogenation, an intimate contact between the two metals is necessary in order to carry out the reaction efficiently. During the reaction, the amount of bimetallic particles decreased and unalloyed Pt considerably increased, which led to a partial deactivation of the catalyst. Selective hydrogenation of acrolein to allyl alcohol with molecular hydrogen is extremely difficult. Silver catalyst is used typically for oxidation reactions rather than for hydrogenation, however an important improvement of selectivity to allyl alcohol is possible, when bimetallic $AgIn/SiO_2$ catalysts are used [18]. Even in a strongly reducing atmosphere In remains to some

extent positively charged. Concerning the silver centre, comparable redox behavior could not be observed.

Biomass, not appropriate for human and animal feeding, became a desired renewable raw material and energy source. The processing is focused to economical production of more valuable substances, chemicals, energy carriers such as, hydrogen, methane or liquid fuel or to produce easily transportable electric energy. The alcohols are important chemicals and lower alcohols, first of all ethanol, can be directly used as a fuel. The anaerobic fermentation of sugar is a well known process for ethanol production. However, the use of sugar or starch for fuel production decreases the food output of the agriculture, raises food prices and is economically, environmentally and socially disadvantageous. Present research aims to establish scientific bases of a new technological and material platform for alcohol production.

Chemicals and fuels can be produced from biomass by thermochemical, biochemical and catalytic technologies, and combination thereof. With exception of the sugar route most of the important technological platforms provide fatty acids or volatile fatty acids (VFAs) [19]. The increasing demand for biofuel initiates research to efficiently convert VFAs (first of all acetic acid) to alcohols instead of deeply reduced, gaseous alkanes or biogas. The traditional technology for obtaining fatty alcohols involves esterification of the acid and catalytic hydrogenolysis of the ester at elevated temperature and high pressure to two alcohols over old fashioned Adkins catalyst. The technology of fatty alcohol production cannot be directly adopted for the partial hydrodeoxygenation (HDO) of VFAs to get lower alcohols. Recently we discovered novel highly efficient bimetallic supported catalysts, which were active and selective in the HDO of octanoic acid to octanol at moderate pressure and temperature [6]. The catalysts contained indium and another metal of hydrogenation activity, such as, copper or nickel, on oxide support [20, 6]. Research is needed to study in details these novel catalyst compositions and catalytic process.

2. PREPARATION AND TESTING OF CATALYSTS

Copper (CuZ) and nickel (NiZ) zeolites A, P, X and Y were prepared from NaA, NaP, NaX and NaY commercial products by conventional aqueous ion-exchange using Cu (acetate)$_2$ and Ni (acetate)$_2$. The obtained samples had a metal content of about 7–16 wt. %. Copper or nickel zeolite preparations e.g. with 10 wt. % metal content are marked as 10CuZ or 10NiZ where Z denotes A, P, X, Y zeolite.

Alumina-supported Cu and Ni catalysts were prepared on γ-Al_2O_3 using impregnation with NH_4OH solution of Cu (acetate)$_2$ and Ni (acetate)$_2$, then dried and calcined at 550 °C for 3 hours to decompose the acetate to oxide and 9Cu/Al_2O_3 and 9Ni/Al_2O_3 were obtained, i.e. preparations containing 9 wt. % copper and 9 wt. % nickel.

Composite catalysts were prepared by adding indium (III) oxide powder to the CuZ, NiZ, Cu/Al_2O_3 and Ni/Al_2O_3 samples and grinding the mixture in agate mortar.

A commercial, conventionally used Adkins catalyst (consisting of 72 wt. % $CuCr_2O_4$ and 28 wt. % CuO) was tested for comparison with the novel catalyst preparations.

X-ray powder diffractograms (XRD) were recorded using XRD cell for measurements at room temperature and for *in situ* measurements in gas flow (hydrogen) at elevated temperatures. The mean crystallite size of the copper particles was estimated by the Scherrer equation.

Catalytic hydroconversion of acetic acid (CH_3COOH), octanoic acid ($C_7H_{13}COOH$), octanal ($C_7H_{13}CHO$) /as intermediate compound/, and of octanol ($C_8H_{13}OH$) /as product/ were investigated. Catalyst was generally pretreated in hydrogen flow in the high-pressure fixed bed flow-through catalytic reactor at 450 °C and 21 bar. The reactions were carried out at 21 bar total pressure in a flow of acetic acid or octanoic acid/H_2/He mixtures. The reaction

temperature and the H_2 partial pressure were varied in the ranges of 200-380 °C and 3.6-21.0 bar, respectively.

The reaction was allowed to run for one hour at each temperature to attain steady state and for a second hour to collect reactor effluent for analysis. The reactor effluent collected in the second hour of catalytic run was depressurized, and cooled to room temperature. The product mixtures were analyzed by gas chromatograph (GC) equipped with a capillary column and a flame ionization detector. The non-condensing products (CO, CO_2, CH_4 and light hydrocarbons) were analyzed using an on-line GC with capillary column and thermal conductivity detector.

Product compositions are expressed in weight percents and plotted in stacked area graphs where the distance between two neighboring curves represents the concentration of a given component at a given temperature.

3. RESULTS AND DISCUSSION

A major 21st century goal for academia, government and industry should be the efficient and economical utilization of biomass resources principally for production of transportation fuels and chemicals. Some of our present works focused on the hydroconversion of sunflower oil [21, 22] or octanoic acid [5] to aliphatic paraffins (C_{17} or C_{18} and C_7 or C_8). The reaction proceeded in consecutive steps of fast hydrogenolysis to carboxylic acids and propane, and hydrodeoxygenation (HDO) of the carboxylic acid intermediates. Furthermore, the increasing demand for biofuel initiates research to efficiently convert short chain carboxylic acid produced from biomass by biological destruction (first of all acetic acid) to alcohol preserving the original chain length. Such a process however needs novel, well engineered, tailor-made, bi- or multi-component catalysts similarly to the conventional, old-fashioned Adkins or HDS catalysts.

The copper catalyses selective addition of hydrogen to carbon-oxygen bonds but scarcely the hydrogenolysis of the carbon-carbon bonds in alcohols produced by hydrogenation of triglycerides. From the early 30s up to now the chemical industry transforms triglycerides, primarily vegetable oil, by catalytic hydrogenation to fatty alcohols [1]. For fatty alcohol production chromium-containing copper (Adkins) catalysts are used. The use of toxic chromium involves environmental and health hazards, therefore, research was continued to develop new, environmental benign hydrogenation catalysts for the process. An obvious approach of the alcohol selectivity problem is to use low-activity supported copper catalyst, containing copper in high dispersion as possible. Furthermore, in order to increase the conversion and improve selectivity at moderate pressure the reaction temperature must be increased and/or a catalyst modifier must be used that is less hazardous than chromium.

The regularly structured crystalline microporous aluminosilicates like the zeolites were supposed to be ideal supports for the stabilization of highly dispersed copper clusters or a perfect dispersion of Cu-atoms [23, 24]. However, the conversion of octanoic acid (OA) over more silicious and consequently hydrothermally stable, reduced Cu-zeolites (e.g. mordenite and ZSM-5 having low copper contents because of their low aluminum content) was low, i.e. only 6-7 wt. % at 380 °C and 21 bar. Zeolites A, X and P having the possible lowest Si/Al ratio (around 1), consequently containing the highest number of charge compensating cations as possible, fully ion-exchanged with copper cations already show much higher activities in the reduction of octanoic acid (see Table 1.). However, it is well-known that Al-rich zeolites, shown above, do not preserve their structure in the H-form inevitably generated when the Cu^{2+} cations are reduced with H_2. The 14CuP, 15CuX and 16CuA preparations have similar chemical composition and show similar structural instability under the conditions of activation and of OA hydroconversion [20, 25]. In addition, H-zeolites formed during the

reduction of Cu^{2+} cations having high Brönsted acidity which is very efficient in mono- or bimolecular alcohol dehydration producing alkenes or ethers as undesirable by-products.

The H-zeolite is a solid acid. If the zeolite structure contains protons as charge compensating cations in high concentration the solid acid hydrolyses the zeolite structure. Attempts to substitute the mobile (active) protons with mono- or bivalent metals added in form of salt or vapor were not successful.

In presence of In_2O_3 copper zeolite could be reduced with H_2 without formation of H-zeolite but formation of In^+Z^- [26, 27]:

$$In_2O_3 + 3H_2 + Cu^{2+}Z^- \leftrightarrow 2In^+Z^- + Cu^0 + 3H_2O \qquad (1)$$

where Z^- represents a negatively charged lattice site.

Nevertheless the integrity of the structure of zeolites A, X or P could not be maintained, only small domains of microporous zeolite structures could be preserved upon dehydration/reduction. Nevertheless, the obtained In,Cu composite catalysts embedded in destructed zeolite structure showed much higher activity and octanol selectivity than the simple supported Cu catalysts (see Table 1 and Fig. 1) [20, 25]. This observation gave the base of this research.

Cu-P, -A, -X and -Y-zeolites were pretreated in hydrogen flow at 450 °C before octanoic acid hydroconversion. During pretreatment reduction/dehydration proceed and partly amorphous aluminosilicate supported copper catalysts were formed, which contain copper nanoparticles in sufficiently high dispersion. The diffraction lines, assigned to metallic copper phase were evaluated between 200 and 350 °C (e.g. see diffractograms of 14CuP in Fig. 2a, b). Thus, metal clusters formed when the zeolite structure has been deeply damaged. The size of copper clusters has important relevance. The widths of the diffraction lines assigned to Cu^0 particles are strikingly different for the hollow CuX and the more compact CuA or CuP. The average copper particle sizes in CuX, CuA and in CuP are 26, 7 and 17 nm, respectively.

In CuY, of higher Si/Al ratio than CuX (both of the same faujasite structure), in the stable, faultless microporous faujasite framework with much less lattice aluminum atoms copper cations have free access for the reducing agent hydrogen and the formed copper atoms can migrate to the surface of the zeolite crystals without barrier, so the average copper particle size is much larger, 55 nm. P-, A- and X-zeolite structures collapsed loosing most of the Brönsted acidic sites, whereas Y can preserve its microporous framework containing the charge compensating protons in high concentration.

The activity and selectivity of the catalysts studied can be characterized by the product distributions as function of reaction temperature or time on stream represented in stacked area graphs (e.g. in Fig. 1 for CuP). For a simpler comparison of the catalytic behaviors on the various zeolite based copper catalysts are summarized in Table 1 involving only the main products.

The conversion on CuY of the lowest copper content and of the lowest metal surface are a bit lower than on other Cu-zeolites but the selectivities are highly different. CuY catalyst remained a real microporous H-zeolite without any structural damage loaded copper particles on the outer surface of zeolite crystallites. So, having high Brönsted acid site concentration being equivalent with the formed copper atoms, it is very active in dehydration of the alcohol obtained through the step-by-step reduction of the fatty acid (see Table 1). Contrary, the highly damaged, destructed zeolites of low Si/Al (X, A, P) lost their microporous structure together with the charge compensating Brönsted acidic protons. Consequently, the alcohol intermedier molecules are preserved in much higher concentration depending on the remaining Brönsted acidity characteristic of the parent zeolite structure (zeolite X lattice was the less damaged resulting in high octene yield) (see Table 1).

Adding 10 wt. % In_2O_3 to all four zeolite Cu-catalysts the main effect is that all activities increase (Table 1). Over destructed Cu-zeolites (X, A, P) indium doping is still more efficient,

octanol yields increase strikingly while octene yields significantly decrease. For CuY catalyst having high faultless Brönsted acidity the influence is reflected only in the higher activity, but it remained almost completely selective for octene yield. The great affect of indium admission as co-catalyst seems to be complex. Under pretreatment and reaction conditions active components, copper and indium exist in zerovalent form. Presumably copper-indium intermetallic compounds (most probably Cu_2In) (Fig. 2) are responsible for the activity increase since it has been found that the activity of reduced In_2O_3 (In^0) is negligible under these conditions and the activity of copper is essentially lower. Further question is how and why is suppressed the remaining low dehydration activity as a consequence of the appearance of metallic indium atoms on the surface of support and/or metal particles.

Activity of destructed zeolites in the octanol dehydration reflected by octene yields is different (Table 1) depending presumably on remaining Brönsted acidity. Modification with a large amount of In_2O_3 (added plus 10 wt. % In_2O_3 of the mass of Cu-zeolite catalyst) cocatalyst strikingly increases the activity (cf. e.g. Figs. 1a and A, b and B) preserving it at a permanent level and the high selectivity by eliminating dehydration as a consecutive reaction which is followed by double bond hydrogenation:

$$\text{octanoic acid} \xrightarrow[-H_2O]{+H_2} \text{octanal} \xrightarrow[-H_2O]{+H_2} \text{octanol} \xrightarrow{+H_2} \text{octenes} \rightarrow \text{octane} \qquad (2)$$

When product distribution is plotted against the reaction temperature the efficiency of indium-doping seems to be more significant at lower temperature (Fig.1a, A) and the consecutive nature of this reaction is reflected in Fig.1A showing the concentration change of the octanal intermedier compound.

The moderate decay of activity can be also eliminated by In admission (compare Fig. 1b and 1B).

Summing-up, well dispersed copper particles can be generated on aluminosilicate supports formed by destructive H_2 reduction/dehydration of zeolite CuP, CuA and CuX. Such amorphised type catalysts show high activity and selectivity in the catalytic hydroconversion of carboxylic acids to alcohols. The selectivity for alcohol depends on the original zeolite structure. Zeolite CuA (small pore) seems to be a better catalyst precursor than CuX (large pore), having the same composition but different frameworks consisting of the same building units (linked truncated octahedras). The activity and the alcohol yield of the supported Cu catalysts can effectively be increased by In_2O_3 doping. Appearance of indium metal in the active metallic copper containing phase highly increases the activity and selectivity. It seems likely that indium effectively eliminates the dehydration of octanol to octenes for Cu-zeolite catalysts of low Brönsted acid site concentration.

The catalytic behaviour of zeolite based amorphised catalyst samples significantly depends on the original zeolite structure. Although the destructed zeolite CuA sample has the smallest specific surface area (only 8 m^2/g), its activity is similar to that of CuX, CuP but the octanol selectivity is the highest without indium doping (Table 1) and In admission enhances only the conversion (cf. Figs. 3a and A).

Non-sulfided Ni-catalysts for sunflower oil hydroconversion to green Diesel [21, 22] were proven to be too active and catalysed effectively the side reactions besides desired alkane formation. Indium doping offers itself to attain better selectivity and more moderate reaction conditions over the too active nickel catalysts. In Fig. 3 the octanoic acid hydroconversion over CuA (at 380 °C) and NiA (at 300 °C) catalysts with and without indium doping are compared. The activity differences are reflected by the high reaction temperature difference for attaining comparable activities. On the NiA catalyst fast activity decay can be observed (Fig. 3b) contrary to the other three catalysts (in Figs 3a, A, B). This sample can split the C-C bonds resulting in the hydrodecarbonylation reaction producing chain shortened

alkane (heptane) and CO which is quickly hydrogenated to methane (CO and CH_4 are plotted together with the other products (OP)). Admission of 10 wt. % In_2O_3 results in drastic or rather breath-taking improvement of catalytic behaviour reflected by permanent conversion at high level together with high octanol selectivity. Compared with the Cu-zeolites it is important to mention, that Ni^{2+} cations in the negatively charged zeolite lattice can be reduced only under drastic conditions, at much higher temperature than Cu^{2+}, i.e. above 350 °C. Consequently at low level of nickel cluster formation after partial reduction the crystallinity of the zeolite can be preserved in higher extent. HT-XRD diffractograms confirm this assumption. Such effect can be enhanced by using partially exchanged Ni,Na-A zeolite which contains nickel cations exchanged only to 20 % of the originally present sodium cations. However the catalytic behaviors were very similar for such highly different samples. Consequently, although observing nice effects using the indium co-catalyst loaded Cu- or Ni-zeolites, it seems to be practical to apply more simple and more conventional supports (Al_2O_3, SiO_2, TiO_2, etc.) than amorphous aluminosilicates of zeolite origin which are too complex although very interesting for detailed researches.

ALUMINA SUPPORTED InNi AND InCu COMPOSITE CATALYSTS

Alumina supported Ni-catalysts prepared in two different ways (one of them is a non-pyrophoric Raney type nickel catalyst) were found to catalyze highly selectively the hydrodecarbonylation of fatty acids formed as intermediates of triglyceride hydrodeoxygenation [22]. In order to make clearer the scheme of transformations octanoic acid was used as reactant. Catalysts showed high activity and sufficient decarbonylation selectivity but CO methanation and paraffin hydrogenolysis side reactions producing methane in high concentration are very disadvantageous. Non-pyrophoric Raney nickel catalyst was found to be more active than conventional Ni/Al_2O_3 for the side reactions, too. Although the

Ni contents are nearly the same, in non-pyrophoric Raney-Ni the nickel phase can be found mainly in metallic state in contrary to supported Ni-catalysts, where the oxide phase is dominant in spite of the same reduction treatment. Poisoning with Sn or Pb in order to eliminate the activities for the hydrogen consuming side reactions was not successful. However, applying the experiences obtained with the indium doped destructed zeolite supported copper catalysts addition of large amount of In_2O_3 (36 wt. %) was found to be also completely effective in suppressing side reactions over the non-pyrophoric Raney nickel catalyst (see in Table 2). It governed the process again to a new deoxygenating pathway, instead of the chain-shortening hydrodecarbonylation namely into the step-by-step reduction route of carboxylic acid stopped at alcohol formation. Decreasing the amount of In_2O_3 additive the original reaction pathway is gradually restored producing mainly heptane beside octanol whereas paraffin hydrogenolysis is still effectively eliminated (see low hexane yields obtained over indium doped samples in Table 2). It is a great disadvantage that indium (III) oxide is needed in a very high amount to attain these results. Decreasing the amount of indium oxide the selectivity for the main products (heptane or octanol) is changing inversely, even with 18 wt. % of In_2O_3 55 % heptane and only 15 % octanol is obtained (see Table 2). It is interesting to note, that 4 wt. % indium oxide already increases the alcohol production by two orders of magnitude. The methanation of primary product CO is complete, but hydrogenolysis of heptane to hexane, etc. is highly restricted.

Considering only the mass of active phases, the non-pyrophoric Raney type sample contains nickel mainly in metallic form whereas in the alumina supported sample the oxide phase is dominant. However, this condition does not strictly influence the ratio of active surfaces. Another important fact is that starting with a 50-50 wt. % nickel-aluminum alloy an aluminum oxy-hydroxide supported, finely dispersed NiAl intermetallic phase can also be formed. By heating up to 450 °C during the pretreatment the support is transformed to γ-

Al_2O_3 being similar support as in the case of impregnated sample used for comparison [22]. The structure of the non-pyrophoric Raney-Ni catalyst is not well determined like that of destructed zeolites, so detailed investigations regarding the interactions of indium co-catalyst with the main reducing metal, the nickel is worth to be done only with the simplest alumina supported nickel sample, i.e., with the $9Ni/Al_2O_3$ catalyst.

Octanoic acid hydroconversion on monometallic Ni/Al_2O_3 catalyst shows selective hydrodecarbonylation resulting in heptane formation (Fig. 4b). The activity of Ni/Al_2O_3 depends on Ni content. CO formed beside water in hydrodecarbonylation is completely hydrogenated to methane and some excess methane can also formed in hydrogenolysis of heptane as indicated by formation of lower hydrocarbons (e.g. hexane) similarly for NiA (Fig. 3b). Modification with co-catalyst strikingly increases the activity, maintaining it at a constant level and drastically changing the selectivity (Fig. 4B) by eliminating hydrodecarbonylation as a main reaction and H_2 consuming side-reactions thus governing the process to a different consecutive deoxygenating reaction pathway, i.e., a step-by-step reduction with H_2 and stopping this hydrogenation reaction series at alcohol formation before dehydration to alkenes or dioctylether and saturation of the formed olefines [6]**.** The results are well comparable at the same reaction temperature (already at 300 °C) obtained mainly over the indium doped composite bimetallic catalysts (Fig. 4A, B). Influences of indium doping for both base metal catalysts seem to be very similar only with some shift on the reaction temperature scale.

While the carboxylic acid hydroconversion to alkanes increases with the Ni-content of Ni/Al_2O_3 samples, for In_2O_3 doped samples at constant indium content the conversion can be lower when the Ni-content is above an optimum value (see conversion curves obtained over 3, 9 and $18Ni/Al_2O_3$ samples in [6]). Decrease of nickel loading below 9 wt. % is also disadvantageous resulting in the downfall of conversion and octanol yield followed by an increase of octanal selectivity, because only a lower reduction state can be attained over less

active catalyst [6]. Furthermore, using Ni-free alumina sample containing only the indium co-catalyst significant conversion can be observed at much higher reaction temperature (above 350 °C) and the main product is octanal. Without any metal loading the alumina support can produce only traces of octanal and octanol between 350 and 380 °C.

At a fixed Ni-loading (9 wt. %) decreasing the amount of added indium oxide in a wide range hardly affects the selectivity of the catalyst composites [6]. Hence it seems likely to apply in low concentration the expensive, but strongly efficient In_2O_3 co-catalyst. It can be estimated that both active metal components can be used in about 10 wt. % to attain high carboxylic acid conversion with high and stable octanol yield.

In Fig. 5A and D the catalytic properties of a commercial, conventionally used Adkins catalyst (consisting of 72 wt. % $CuCr_2O_4$ and 28 wt. % CuO) and our bimetallic alumina supported composite ($NiIn/Al_2O_3$) are compared along the increasing reaction temperature under identical conditions. Although both samples are able to produce alcohol from fatty acid with high selectivity, the novel catalyst seems, however, to be more active: 80 % overall conversion of OA on $9Ni/Al_2O_3$ catalyst dopped with 10 wt. % In_2O_3 is already attained at 280 °C while on copper chromite only at 360 °C. Indium free $9Cu/Al_2O_3$ sample shows much poorer catalytic properties (Fig. 5B) than conventional Adkins catalyst (Fig. 5A), however after doping of the highly efficient indium the activity exceeds that of commercial Adkins type copper catalyst (Fig. 5C).

Dioctyl ether formation in bimolecular octanol dehydration on $9Ni/Al_2O_3$ dopped 10 wt. % In_2O_3 samples becomes important only at high octanol yield above 280 °C (Fig. 5D). Monomolecular octanol dehydration appears only above 300 °C. Both these acid catalyzed side reactions may be attributed to alumina. However, these undesirable reactions can be eliminated on highly active and stable $9Ni/Al_2O_3$ + 10 wt. % In_2O_3 catalyst composite applying lower reaction temperature and higher space velocity.

Beside the main metal phase active in hydrogenation, the applied support and its interactions with the indium co-catalyst may be of importance to ensure the advantageous catalytic properties. These interactions may be negligible correlated to the hydrogenation of reactant carboxylic acids under moderate conditions; however, they can become significant at much higher reaction temperature. Product compositions are displayed in Figs. 6 after contacting intermediate product aldehyde (Fig. 6a, b, c) and desired end product alcohol (Fig. 6A, B, C) with alumina support, alumina and In_2O_3, $9Cu/Al_2O_3$ and In_2O_3. Octanal is extremely reactive in aldol type condensation on pure alumina support leading to dimmer formation (Fig. 6a). Active sites for aldol condensation can be effectively deactivated by metallic indium admission while octyl aldehyde is reduced to octyl alcohol and octanol is hardly dehydrated (Fig. 6b).

Octanol can easily be dehydrated to dioctyl-ether and octenes over the alumina support (Fig. 6A). At lower reaction temperature the bimolecular dehydration forming dioctyl ether is dominant. On increasing the temperature the monomolecular dehydration resulting in olefin formation becomes the main reaction pathway. Probably this change of dehydration mechanism is essentially affected by the decreasing alcohol coverage of the surface at increasing temperature. Indium on the surface of alumina effectively suppresses alcohol dehydrations (Fig. 6B).

Using octanal as reactant dioctyl ether yield is very low because of the competing aldol condensation alcohol formation is suppressed on the alumina surface (Fig. 6a). Comparison of figures in the first column of Fig. 6 gives some insight into the role of indium: i., aldol condensation of octanal is greatly suppressed by indium (Fig. 6b), ii., the dehydrations of octanol are suppressed as well by indium suggesting that indium blocks the active sites of the alumina support (Fig. 6b, Fig. 6B) and iii., indium seems to be active in aldehyde reduction, at higher temperature than the main hydrogenating metal, copper (Fig. 6c) or nickel. Correlation

of Fig. 6C and Fig. 5C indicate that the presence of the reactant fatty acid can play an important role to poison the active centers of dehydration together with indium, because octanol can be highly dehydrated over $CuIn/Al_2O_3$ catalyst, i.e., in presence of copper and indium on alumina, but in absence of the organic acid reactant. Fig. 6c demonstrates that copper can promote the reduction with hydrogen of the aldehyde at much lower temperature than indium (Fig. 6b) being more active hydrogenating metal, but the distribution of various components, types of sorption sites and the coverage of organic compounds on each those over the catalyst surface are very important. Summarized it can be stated that indium can deactivate dehydrating active sites, when carbonyl group is present in the reactant (acid or aldehyde adsorption is necessary).

$NiIn/Al_2O_3$ catalyst is more active in octanoic acid hydroconversion than $CuIn/Al_2O_3$ since the conversion and octanol yield curves are shifted by 20 – 30 °C to higher temperatures for $Cu,In/Al_2O_3$ (Fig. 5C, D). However, the product distributions are the same on both bimetallic catalysts. Hence, similarity of catalytically active phases seems probable.

For $9Ni/Al_2O_3$ catalyst at the routine pretreatment temperature, at 450 °C only a small fraction of NiO is reduced and a complete reduction can be attained only at 650 °C (Fig. 7b) [6]. While in $9Cu/Al_2O_3$ catalyst copper oxide is already fully reduced at 200 °C and copper particles of ~20 nm average diameter (∇ in Fig. 7a) are formed and these particles do not change up to 650 °C (and not only up to 450 °C as shown in Fig. 7a). Reduction of admixed In_2O_3 can be observed at much higher temperature, i.e., between 350 and 450 °C (see Fig. 7A and Fig. 7B) detected by disappearence of In_2O_3 diffraction lines (+). In_2O_3 reduction is completed up to 450 °C on all $9Cu/Al_2O_3$ and $9Ni/Al_2O_3$ samples when indium is in liquid form (see Fig. 7). The generated zerovalent indium can already form copper-indium alloy (●) above 350 °C (see Fig. 7A). In the case of this composition copper particles, i.e., the pure metal phase can not be detected below the reduction temperature of In_2O_3 indicating either the

formation of too small Cu^0 nanoparticles not detectable by XRD method or more probably the alloying of the low concentration Cu^0 with small amount of reduced In_2O_3 as shown by the appearance of a new phase (marked with ● in Fig. 7A) which can be assigned to some kind of CuIn alloy. Mainly Cu_2In phase, but Cu_4In and Cu_9In_4 phases may also be present in lower concentration. These phases were determined based on ICDD database [27], the corresponding ICDD numbers are Cu_2In: 42-1475, Cu_4In: 42-1477 and Cu_9In_4: 42-1476. After treatment at 450 °C the $9Cu/Al_2O_3$ sample mixed with 20 wt. % In_2O_3 (which amount is more than necessary to form the Cu_2In intermetallic compound), cooling down the composite sample to R.T. the presence of excess solid metallic indium phase (∗) can be also detected (see Fig. 7A). Frozen indium particles with average sizes of ~130 nm are larger than copper particles indicating higher mobility of indium atoms above the melting point (156.4 °C) than that of copper atoms. $9Cu/Al_2O_3$ + 10 wt. % In_2O_3 composite contains Cu and In nearly in 2:1 atomic ratio, so all amounts of two metals are consumed in formation of the alloy phase (Cu_2In) having an average size of ~10 nm [29].

When less In_2O_3 is added Cu and Cu_2In phases are present simultaneously [29], when indium is in excess it appears as a distinct pure metal phase which can only be detected below its melting point 156.4 °C. Formation of Cu and/or Cu_2In alloy nanoparticles, and appearance of zerovalent indium on the support is evident on the basis of HT-XRD results but the clearing of catalytic properties, i.e., complete understanding of the multiple behaviors of such a complex ensemble of active sites requires further comprehensive investigations.

Regarding the pretreatment conditions of the novel, highly efficient NiIn/alumina composite catalyst, influence of the pretreatment temperature on activity and selectivity in OA hydroconversion in a wide range of 350 and 550 °C can not be observed [6]. In_2O_3 is completely reduced while Ni^{2+} only partly, as shown by HT-XRD patterns in Fig. 7b, B. Melting point of In being 156.4 °C (boiling point is >2000 °C) thus the formed metal should

be in liquid phase which may interact with the environment: can penetrate in the surface of the alumina support and/or can form alloy phase(s) immediately with the appearance of nickel clusters arising later in increasing amounts along increasing reduction temperature. At the routine pretreatment temperature, at 450 °C only a small part NiO can be reduced [6, 21] and a complete reduction can only be attained at 650 °C (Fig. 7b). After a similar procedure when the treatment is carried out at 650 °C instead of 450 °C (see Fig. 7B) and cooling to R.T. In^0 diffraction lines can not be anymore detected and a new line /marked with asterisk (∗)/ at 43.2° appears in the diffractogram which can be assigned to some kind of InNi alloy, mainly to $InNi_2$ phase, but $InNi_3$ and $InNi_4$ phases can be also present in lower concentration similarly to the behaviour of Cu-catalysts [30]. It can be concluded: if the catalyst contains enough reduced metallic nickel clusters and the total mass of indium is in zerovalent state, InNi alloy is formed and In^0 is not detectable. Furthermore, it was proven that the appearance of zerovalent indium is necessary to octanol production**.** This requirement is already satisfied by a pretreatment temperature higher than 350 °C.

Metallic nickel phase can be detected in partly reduced monometallic Ni/Al_2O_3 catalysts (Fig. 7b) [21]. Ni^0 particles formed are real nanoclusters having average size in the range 5-8 nm which do not change when the temperature is elevated. The formation of NiIn alloy on the active surface of catalysts can be ascertained on the basis of HT-XRD results (Fig. 7B). The catalytic behavior of $InNi/Al_2O_3$ catalyst in a wide pretreatment temperature range does not change. Presumably the active InNi intermetallic surface can be established with small masses of indium and nickel and further growing of the bulk phase hardly affects the active surface.

OUTSTANDING EFFICIENCY OF INDIUM AS CO-CATALYST COMPARED TO ITS NEIGHBOURS IN THE PERIODIC TABLE

Indium is a very soft, malleable and easily fusible post–transition metal chemically similar to gallium and thallium, and shows the intermediate properties between the two metals. Melting point and boiling point trends are just opposite, where indium has a middle position. Beside chemical properties these physical characteristics may be important in evolution of copper or nickel co-catalysts of outstanding efficiency, e.g., mobility of reduced metal. Appearance of various alloys or intermetallic compounds (some are shown in Figs. 2 and 7) can play important role in formation of the catalytically active centre on the surface. HT-XRD method was proven to be very useful to observe the phase changes of the main mass of indium however the catalytically active sites are in very low concentration. The first results of HT-XRD investigations are shown in Fig. 8 for 10 wt. % In_2O_3, Ga_2O_3, Tl_2O_3, CdO or SnO doped $9Cu/Al_2O_3$.

In_2O_3 is reduced to metal between 350 and 450 °C (Fig. 8d) contrary to Ga_2O_3 which can be reduced only at much higher temperature, between 550 and 650 °C (Fig. 8c). It is important to emphasize that reduction of copper and indium oxides does not take place parallel, which can give better opportunity for alloy or intermetallic phase formation (copper particles are formed at lower temperature than metallic indium). Gallium oxide reduction starts at much higher temperature when the formation of copper particles is accomplished. Both post-transition metals can form some kind of alloys or intermetallic phases with copper (e.g. Cu_2In) indicated by the diffraction line (●) appearing at lower Bragg angle than the more intensive diffraction line of copper (∇). Cu_2In phase (Fig. 8d) seems to be stable, the line is preserved up to 650 °C similarly to Ni_2In (Fig. 7B). In the case of the Ga doped sample the similar signal shows maximum intensity between 550 and 600 °C (Fig. 8c). Above 600 °C

the intensity of this line significantly decreases parallel with the formation of pure Cu phase. This observation suggests that gallium should be more volatile than indium although its boiling point is higher, but its melting point is lower. These HT-XRD results suggest that gallium may be similarly efficient co-catalyst as indium, but the pretreatment temperature is limited by 550 °C (Fig. 8c).

Cadmium, the left hand side neighbour of indium in periodic system can produce similarly intermetallic compounds like indium or gallium, but the signal can be detected only at 350 °C with very low intensity (Fig. 8a). However, this line disappears when the temperature is increased, because cadmium is volatile, as found in solid state ion-exchange experiments [31]. Consequently cadmium doped sample can be reduced and used only up to 350 °C.

The HT-XRD diffractograms of tin doped sample shown in (Fig. 8b) demonstrate that although SnO can be reduced completely to metallic tin up to 550 °C with similar physical properties as indium (e.g. melting point is 232 °C), surprisingly no any formation of alloys or intermetallic compounds can be observed in a wide range of pretreatment temperature: copper and tin can be detected in separate phases in this composite. Thallium (III) oxide showed similar behaviour during the HT-XRD measurement without any trace of formation alloys or intermetallic compounds**.**

Catalytic test results obtained for the doped copper loaded alumina catalysts are summarized in Fig. 9 representing the changes of octanoic acid hydroconversion depending on the reaction temperature. Conversion curves plotted with dashed and with dotted lines relate to $9Cu/Al_2O_3$ and $9Cu/Al_2O_3$ +10 % In_2O_3 catalysts in Fig. 9b and 9d as reference points (full figures can be find in Fig. 5B and C). Fig. 9c perfectly overlaps Fig. 5B which means that the admission of Ga_2O_3 has no any influence to the catalytic behavior after pretreatment at 450 °C. This observation is accordance with the fact that Ga_2O_3 can be reduced only at

higher temperature. However reducing at 550 °C gallium should be present totally in metallic form (Fig. 8c), but instead of improvement of catalytic properties, essentially lower conversions were measured (Fig. 9d). Gallium atoms deactivate partly the surface of copper particles and the bimetallic particles detected in the diffractograms of Fig. 8c do not improve the catalytic behavior.

Cadmium can also form bimetallic phase in a small extent, and cadmium doping can increase the activity and improve the alcohol selectivity (Fig. 9a). The problem is here, that it is easy to loose the cadmium co-catalyst due to its high volatility. SnO can be completely reduced above 450 °C, but SnCu alloy formation can not be detected by XRD method. Presence of tin atoms causes an effective poisoning together with unfavourable change in the selectivity producing chain shortened heptane instead of C_8 compounds. Probably copper surface is fully poisoned, perhaps covered with tin atoms and the observed conversion is catalysed only by tin. Thallium showed similar changes in the XRD cell as tin. This element and most of its compounds are highly poisonous, hazardous materials, so the catalytic tests were omitted with thallium doped composite.

It can be concluded that indium as co-catalyst has an unique quality which results in creating highly advantageous CuIn or NiIn bimetallic composites. Appearance of bimetallic phases seems to be essential that an improvement in qualities of copper or nickel catalyst could be attained (with In, or Cd). However the formation of some alloys or intermetallic compounds is not enough to come to the desired catalyst (see gallium). It can be supposed that the highly active species are presumably present in very low concentration, i.e., in form of very thin layers or small clusters on the active metal surface and their identification seems rather difficult.

Commercial Adkins catalyst has very high copper content which is present under the reaction conditions in metallic form (see Fig. 10A). Adding 10 wt. % In_2O_3 the catalytic

behaviour drastically changes (cf. Figs. 10a and b) becoming totally similar to that of $InCu/Al_2O_3$ supported composite catalyst. In the HT-XRD patterns influence of 10 wt. % In_2O_3 admission can not be detected (Fig. 10B). Admission of 50 wt. % In_2O_3 results in a radical change of the diffractograms. Only Cu_2In phase can be detected alone which points to the formation of this characteristic phase the presence of which is coupler with outstanding catalytic behaviour.

HYDROCONVERSION OF ACETIC ACID TO BIOETANOL AND ETHYLACETATE

Numerous biomass conversion pathways, biomass degradation platforms generate carboxylic acids. Regarding the need of transportation and the industrial sectors for chemicals, the selective catalytic hydroconversion of bio-acids to alcohols, ethers, and esters is a process of high commercial interest. Up to 150 °C the distillate of the bio-oil, obtained from lignocellulose pyrolysis contains lower carboxylic acids and aldehydes in relatively high concentration. Fuel alcohol can be obtained by selective reduction of these components. Instead of the less advantageous thermochemical routes, a novel and favorable microbiological destruction /MixAlco/ process is elaborated [19]. In principle, the biogas process is suggested to be stopped after the rapid anaerobic acidogenic digestion stage to produce volatile fatty acids (VFA), mainly acetic acid [32-33], not followed by the slow methanogenesis step. The overall chemical reaction without any loss of biomass conducted by species of anaerobic bacteria, including members of the genus Clostridium may be represented as:

$$C_6H_{12}O_6 \rightarrow 3\ CH_3COOH \qquad (3)$$

The efficiently selective hydrogenation of such volatile fatty acids (VFAs, e.g. acetic acid) to alcohols in a continuous flow system working in vapor phase under mild conditions seems to be still a problematic step.

As it has been shown indium doping of supported Ni or Cu catalyst proved to be highly efficient for reduction of the long chain fatty acids to aliphatic alcohols opening a novel route for catalyst development. The same catalyst systems seem promising for the selective reduction of VFAs, short chain carboxylic acid homologues to alcohols. Acetic acid (AA), the most easily available platform material obtainable from degradation of non edible biomass, as a model reactant is of great importance.

Highly dispersed copper particles can be produced on amorphous aluminosilicate by dehydration/H_2-reduction of low-silica Cu-zeolites. The obtained Cu/aluminosilicate preparations have high activity and selectivity also in the hydroconversion of biomass-derived carboxylic acids (e.g. acetic acid) to alcohols, aldehydes and esters. The catalytic properties depended on the original zeolite structure as it has been found for octanoic acid. Hydrogenation activity and selectivity of the supported Cu/aluminosilicate catalysts can be significantly modified by In addition. The catalytic activity and selectivity of different catalyst compositions are reflected by the product distribution as function of temperature (see Fig. 11). Only traces of gaseous products (ethylene, CH_4, CO and CO_2) were detected on Adkins and indium doped catalysts. Main products formed from AA over all In-free Cu-zeolite catalysts were ethanol and ethyl acetate (see e.g. on CuA in Fig. 11a). The acid is reduced first to acetaldehyde and then to ethanol. Depending on the reaction conditions, fractions of the reactant acid and the product alcohol formed ethyl acetate according to the Fischer esterification mechanism. In addition, ethyl acetate can be also formed directly from two acetaldehyde molecules according to the Tishchenko reaction.

With exception of 16CuA, all the other zeolite-based catalysts were significantly more active than commercial chromium-containing Adkins catalyst and demonstrate different selectivity being the main product ethyl acetate unlike ethanol. Such a direct reaction route to the valuable ester product can be economically more attractive and environmentally benign

[34]. When fatty acids of longer chains, e. g. OA, were reduced over the same catalysts, the addition of In_2O_3 to the catalyst drastically increased the conversion and octanol yield. Using AA as reactant, the In_2O_3 addition changed the selectivity and the conversion as shown for 16CuIn/A (Fig. 11b). Acetaldehyde appeared in high concentration at lower conversions and the ethyl acetate yield was low. The product distribution could be hardly influenced by increasing the amount of the In_2O_3 modifying agent between 5 and 36 wt. %. The greatest change takes place at low loading, below 2 wt. % suggesting that indium is effective even in low concentration.

The catalytic activity and selectivity of the alumina supported catalyst preparations are characterized by the product distribution as a function of reaction temperature and are shown in Figs. 11d, e and f. Main valuable products formed from acetic acid (AA) are ethanol and ethyl acetate. As by-products acetaldehyde, acetone, ethane, methane, carbon dioxide, carbon monoxide and water were determined in various amounts depending on the composition of the catalysts. Carboxylic acid is converted first to aldehyde then to alcohol, fractions of the reactant acid and the products can form ethyl acetate according to the Fischer and/or Tishchenko esterification mechanism. From acetic acid after AA-anhydride formation decarboxylation takes place resulting in formation of acetone and CO_2. Ethanol can be easily dehydrated in a monomolecular way to ethylene or to diethyl-ether. Similarly to long chain fatty acids two hydrodeoxygenation routes [10] can be distinguished: (i) consecutive, step-by-step reduction of carboxyl group or (ii) one step hydrodecarbonylation resulting in carbon monoxide and water.

X-ray diffraction patterns recorded and evaluated proves that in the novel $InNi/Al_2O_3$ composite catalysts, activated at 450 °C in H_2 flow before the reaction, In_2O_3 is reduced and indium metal far above its melting point (156.4 °C) is present under the reaction conditions and finely dispersed bimetallic $InNi_2$ particles are formed (Figs. 7b and B). Consequently, the

appearances of these two characteristic components in the samples containing initially admixed In_2O_3 are responsible for the drastic changes of catalytic properties (cf. Figs. 11e and f). In general, the modification by indium changes the hydrogenation activity of the nickel catalyst for the C−O or C=O bonds and controls the extent of side reactions.

Unlike octanoic acid for fatty acids of short carbon chain, e.g. acetic acid (AA) as reactant contacted with Ni/Al_2O_3 or $InNi/Al_2O_3$ catalyst and (Figs. 11e and f) beside alcohol the ester is a typical product, as well. However, neither ether nor alkene formation can be detected contrarily to octanoic acid. Alkyl-chain lengths of reactants affect the adsorption capabilities which determine the coverage of the reactant or product compounds on the same active surface and thus results in significantly different catalytic activities and product distributions.

$9Ni/Al_2O_3$ catalyst (Fig. 11e) was similarly active as the commercial chromium-containing Adkins catalyst (Fig. 11c) but shows different selectivity being the main product ethyl acetate unlike ethanol. Octanoic acid hydroconversion on monometallic Ni/Al_2O_3 catalyst shows selective hydrodecarbonylation resulting in heptane formation as main product (Fig. 4b). Using acetic acid as reactant similar transformation can proceed also, but in much lower extent as shown in Fig. 11e by methane formation at increasing reaction temperature when from one acetic acid molecule one methane can form by hydrogenation of carbon monoxide evolved in hydrodecarbonylation and a second one from the remaining methyl group. However, the other reaction path the step-by-step reduction of acetic acid to ethanol seems to be dominant, which can come to end immediately with a fast esterification of reactant acid and the product alcohol resulting low ethanol yield as shown in Fig. 11e. At the same time a quite different parallel reaction path for the considerable ethyl acetate production can be easily conceivable from the reactive intermedier, acetaldehyde (Tishchenko reaction as a special case of the Cannizzaro reaction). Alumina support can play a determining role in

ester formation either Ni or $InNi_2$ particles are present. Here is an exciting room for future research for understanding the reaction mechanism of ethyl acetate formation.

Modification by adding 10 wt. % In_2O_3 co-catalyst to Ni/Al_2O_3 catalyst highly increases the activity and strikingly changes the selectivity (cf. Figs. 11 e and f). Hydrodecarbonylation is completely eliminated (methane is not formed) governing thus the process clearly to the consecutive deoxygenating reaction pathway, i.e., to a step-by-step reduction with H_2 and stopping this hydrogenation reaction series at ethanol formation allowing esterification to a limited extent, however, ester can be formed from intermediate aldehyde, too, as mentioned before. The boiling points of these two main products are nearly the same thus being their separation rather expensive. Using the product mixture as fuel the separation is not necessary. Compared with the commercial, conventionally used Cu-chromite (Adkins catalyst) catalyst (Fig. 11c) and the bimetallic alumina supported composite ($InNi/Al_2O_3$) the novel catalyst system (Fig. 11f) seems to be essentially more active and selective for producing ethanol.

Beside the metal phase being active in hydrogenation reactions, the support applied and its interactions with the indium co-catalyst may be of great importance to ensure the advantageous catalytic properties. Furthermore Ni and/or In free alumina can catalyze undesirable side reactions. Fig. 11d demonstrates the catalytic behavior of γ-alumina support with reactant AA. It has some activity at higher reaction temperatures than the $InNi/Al_2O_3$ composite catalyst on which complete hydroconversion of AA can be attained in this temperature range. Above 300 °C the support can selectively catalyze acetone formation proceeding via bimolecular dehydration of AA followed by decarboxylation. No products of the desired consecutive AA reduction can be detected. Consequently all the products shown in Fig. 11e are formed only over nickel particles. Contrary the liquid indium metal (working far above its melting point) presumably well dispersed on alumina support shows significant hydrogenating activity producing all the compounds observable in consecutive AA reduction

steps as main products but by 80-100 °C higher reaction temperature than over the $InNi/Al_2O_3$ composite (not shown in Fig. 11). Besides this, partition of the original activity of the alumina support is still preserved in presence of indium since significant amounts of acetone and CO_2 are produced. It means that indium atoms at this concentration can deactivate only a fraction of such active sites all over the surface of alumina support.

On comparing hydroconversion of octanoic or ethanoic acids over $InNi/Al_2O_3$ composite catalyst (cf. Figs. 4B and 11f at 300 °C) similar conversions can be observed at the same mass feed rate of acids suggesting that the *molecular* reduction rate of the carboxylic group on the bimetallic surface (perhaps only to a formyl group) is higher for lighter carboxylic acid than for heavier one. In addition the product compositions are different: in hydroconversion of octanoic acid either aldehyde or ester can not be detected but some alcohol dehydration takes place, while for acetic acid both ester formation is considerable and aldehyde formation can be observed but no dehydroxylation.

The activity dependence on the reactant partial pressures indicates the rate-controlling Langmuir-Hinshelwood kinetics (not shown).

Combining relatively simple pyrolytic (or biochemical) technologies resulting in production of acetic acid with the catalytic transformations shown, bioethanol and chemicals, such as ethyl acetate, can be obtained from biomass, e.g. from lignocellulose.

Regarding the continuation of this research the main question is how the second metal, the indium modifies the activity of the supported hydrogenation metal and the surface properties of the oxide support? It is essential to gain basic knowledge of the conversion kinetics and the mechanisms at molecular level for engineering effective catalyst composition and catalytic process. What are the elementary reactions of the HDO process and what is the kinetics of the reaction? What are the rate determining step and the most abundant surface intermediate of the consecutive HDO reaction? What is the molecular mechanism of the

elementary reaction steps? How to prepare well tailored catalyst of required selectivity? What is the structure of the active site? What factors determine the activity, selectivity and catalyst stability?

4. CONCLUSIONS

Indium doping of supported Cu or Ni catalysts has been discovered to be highly efficient in reduction of long or short chain fatty acids with hydrogen opening a novel route for catalyst development. Hydrogenation of carboxylic acid resulting in selectively produced alcohol can similarly be increased by In_2O_3 doping over Cu as well as over Ni supported catalysts. Presence of metallic indium or rather alloying copper and nickel particles can effectively stop the step-by-step catalytic reduction after alcohol formation and hinders the consecutive mono- or bimolecular dehydration of product. High conversion with high alcohol selectivity can be attained in a wide loading range of Cu or Ni and In on various supports. During the pretreatment in hydrogen flow copper oxide is reduced to metallic nanoparticles at lower temperature than In_2O_3, but equally below the pretreatment temperature (450 °C). These differences are not reflected by any change of catalytic behaviour in a wide range of Cu and In content. Contrary, nickel cations can be reduced only at higher temperature than In_2O_3, but the catalytic behaviour is also independent of the pretreatment temperature i.e., on degree of reductions. Minute amounts of the active metals are participating in catalytic transformations.

Appearance of Cu_2In and Ni_2In alloy phases on the surface of metal particles results in significant increase of hydrogenation activity, however, the presence well–dispersed indium atoms or clusters in liquid state on the surface of support seems to be determinative for the selective poisoning the alcohol dehydration capability of the support. The beneficial properties of indium acting as co-catalyst seems to be unique compared to

its neighbors in the periodic table (Ga, Tl, Cd and Sn) similarly to its outstanding role in electronic industry.

The activity dependence on the reactant partial pressures reveals Langmuir-Hinshelwood kinetics with rate controlling surface reaction over the composite catalyst.

ACKNOWLEDGEMENT

The authors wish to express their appreciation to Mrs. Ágnes Farkas Wellisch for her technical assistance.

REFERENCES

1. H. Adkins, R. Connor, J. Am. Chem. Soc. 1931, 53, 1091-1095.
2. R. Prins, V.H.J. de Beer, G.A. Somorjai, Catal. Rev. Sci. Eng. 1989, 31, 1-41.
3. P. Simacek, D. Kubicka, G. Sebor, M. Pospisil, Fuel 2009, 88, 456-460.
4. D. Kubicka, L. Kaluza, Appl. Catal. A 2010, 372, 199-208.
5. L. Boda, Gy. Onyestyák, H. Solt, F. Lónyi, J. Valyon, A. Thernesz, Appl. Catal. A 2010, 374, 158-169.
6. Gy. Onyestyák, Sz. Harnos, D. Kalló, Catal. Com. 2011, 16, 184-188.
7. F. Lónyi, H. Solt, J. Valyon, A. Boix, L.B. Gutierrez, J. Mol. Catal. A 2011, 345, 75-80.
8. J.A.Perdigon-Melon, A. Gervasini, A. Auroux, J. Catal. 2005, 234, 421-430.
9. M. Chen, J. Xu, Y.M. Liu, Y. Cao, H.Y. He, J.H. Zhuang, Appl. Catal. A 2010, 377, 35-41.
10. M. Chen, J.L. Wu, Y.M. Liu, Y. Cao, K.N. Fan, Catal. Com. 2011, 12, 1063-1066.
11. H. Lorenz, W. Jochum, B. Klötzer, M. Stöger-Pollach, S. Schwarz, K. Pfaller, S. Penner, Appl. Catal. A 2008, 347, 34-42.
12. Y. Men, G. Kolb, R. Zapf, M. O'Connell, A. Ziogas, Appl. Catal. A 2010, 380, 15-20.

13. A. Jahel, P. Avenier, S. Lacombe, J. Olivier-Fourcade, J.C. Jumas, J. Catal. 2010, 272, 275-286.
14. W.M. Hexana, N.J. Coville, Appl. Catal. A 2010, 377, 150-157.
15. S.B. Kogan, M. Herskowitz, Catal. Com. 2001, 2, 179-185.
16. S.A. Bocanegra, A.A. Castro, O.A. Scelza, S.R. de Miguel, Appl. Catal. A 2007, 333, 49-56.
17. F.A. Marchesini, C.A. Querini, E.E. Miró, F.G. Requejo, J.M. Ramallo-López, Catal. Com. 2008, 10, 355-358.
18. F. Haass, M. Bron, H. Fuess, P. Claus, Appl. Catal. A 2007, 318, 9-16.
19. H.N. Chang, N.J. Kim, J. Kang, C.M. Jeong, Biotechn. Bioproc. Eng. 2010, 15, 1-10.
20. Sz. Harnos, Gy. Onyestyák, J. Valyon, M. Hegedűs, Z. Károly In Proceedings of 10th Pannonian International Symposium on Catalysis; M. Derewinski, B. Sulikowski, A. Wegrzynowicz; Ed; Polish Zeolite Association and Institute of Catalysis and Surface Chemistry, PAS: Kraków, 2010; pp. 334-341.
21. Sz. Harnos, Gy. Onyestyák, D. Kalló, Reac. Kinet. Mech. Cat. 2012, DOI: 10.1007/s11144-012-0424-6.
22. Sz. Harnos, Gy. Onyestyák, Á. Szegedi, D. Kalló, Fuel 2012, (in print)
23. Beyer, H., Jacobs, P.A., Uytterhoeven, J. B. J. Chem. Soc. Faraday Trans. 1 1976, 72, 674-685.
24. R.G. Herman, J.H. Lunsford, H. Beyer, P.A. Jacobs, J.B.J. Uytterhoeven, J. Phys. Chem. 1975, 79, 2388-2394.
25. Sz. Harnos, Gy. Onyestyák, D. Kalló, Micropor Mesopor Mat. 2012**,** DOI: 10.1016/j.micromeso.2012.03.011.
26. H.G. Karge, In: Progress in zeolite and Microporous Materials (H. Chon, S.K. Ihm, Y.S. Uh, Eds.) Stud. Surf. Sci. Cat. 105C (1997) 1901.

27. H.K. Beyer, R.M. Mihályi, Ch. Minchev, Y. Neinska, V. Kanazirev Micropor. Mater. 1996, 7, 333-341.
28. B.D. Cullity In Elements of X-ray Diffraction 2nd edition, Addison-Wesley Publ Co.: Reading, MA, 1978, pp
29. Gy. Onyestyák, Sz. Harnos, D. Kalló, Catal. Com. 2012, (in print)
30. Z. Bahari, E. Dichi, B. Legendre, J. Dugue, Thermochim. Acta 2003, 401, 131-138.
31. Gy. Onyestyák, F. Lónyi, J. Valyon, J. Therm. Anal. Calor. 2005, 79, 561-565.
32. M.T. Holtzapple, C.B. Granda, Appl. Biochem. Biotechnol. 2009, 156, 525-536.
33. V. Pham, M.T. Holtzapple, M.El-Halwagi, J. Ind. Microbiol. Biotechnol. 2010, 37 1157-1168.
34. Atkins, M.P., Top. Catal. 2003, 24, 185-186.

Table 1. The yields of main products of octanoic acid hydroconversion (weight %) at 380 °C, WHSV=2 h^{-1} and 21 bar over various zeolite base catalysts.

Catalyst	Octane	Octenes	Octanal	Octanol	Conversion
7CuY	1.3	20.8	0.9	2.2	41.7
7CuY + 10 % In_2O_3	**3.3**	**49.6**	**1.3**	**2.1**	**84.4**
15CuX	3.9	35.3	1.5	7.3	62.0
15CuX + 10 % In_2O_3	–	**32.1**	**4.5**	**31.1**	**87.8**
16CuA	–	4.6	5.3	42.0	62.7
16CuA + 10 % In_2O_3	–	**2.7**	**6.6**	**63.0**	**85.4**
14CuP	–	16.4	3.7	25.1	58.7
14CuP + 10 % In_2O_3	–	**8.4**	**5.3**	**61.1**	**88.67**

Table 2. The yields of main products of octanoic acid hydroconversion (wt. %) at 300 °C, WHSV=3 h^{-1} and 21 bar in 5 h time-on-stream over a non-pyrophoric Raney nickel type catalyst (NPR27Ni) modified with various amounts of In_2O_3.

Catalyst	Hexane	Heptane	CH_4	Octanal	Octanol	Conversion
NPR27Ni + 0 % In_2O_3	4.2	32.7	9.6	-	0.1	68.2
+ 4 % In_2O_3	0.9	57.6	8.3	0.8	10.6	90.1
+ 18 % In_2O_3	0.3	55.1	7.6	0.5	14.9	89.6
+ 36 % In_2O_3	0.02	10.0	1.2	1.6	57.9	83.2

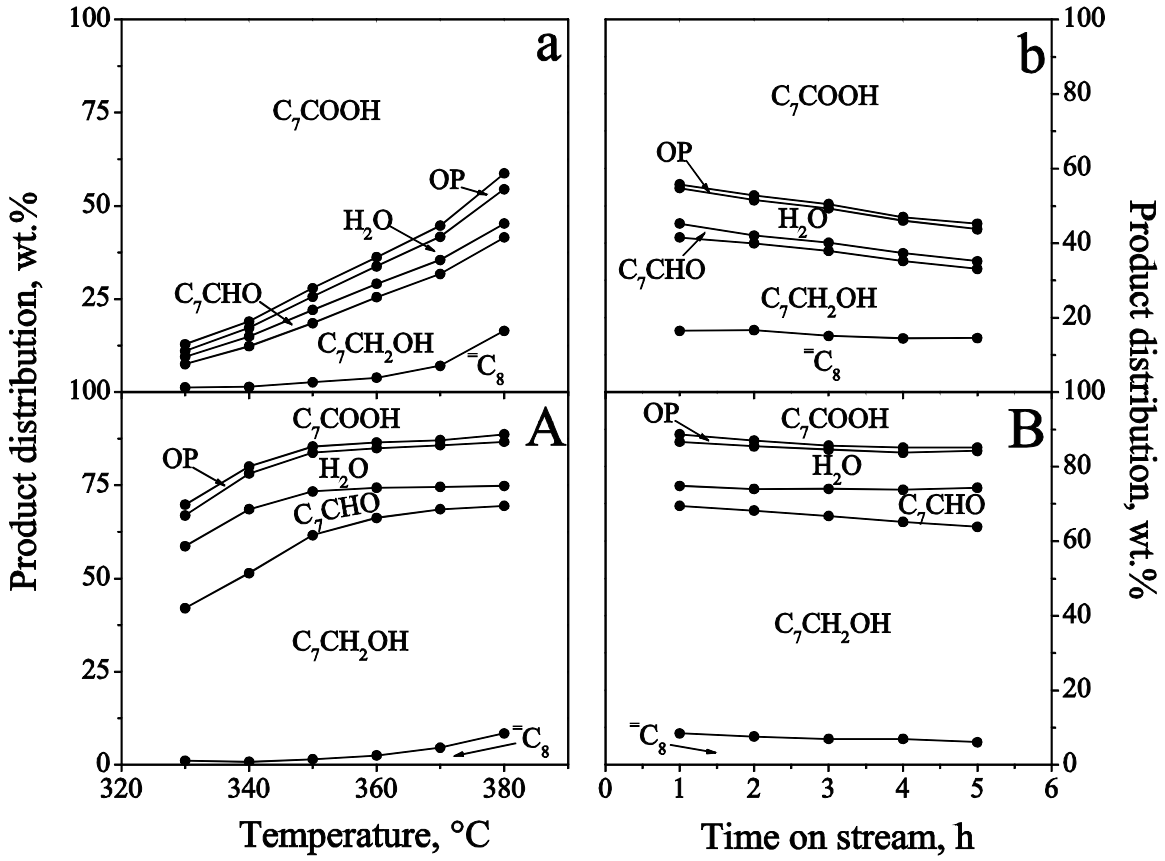

Figure 1. Octanoic acid hydroconversion over 14CuP (a; b) and doped with + 10 wt. % In_2O_3 (A; B) catalysts are characterized by distributions of main products as a function of reaction temperature (a; b) and the time-on-stream (A; B) at 21 bar total pressure. The temperature was kept at 380 °C in the case of time-on-stream measurement. The WHSV of OA was 2.0 h^{-1}. Legends: $^{=}C_8$ octenes; C_7CH_2OH octanol; C_7CHO octanal; H_2O water; C_7COOH octanoic adid; OP other products.

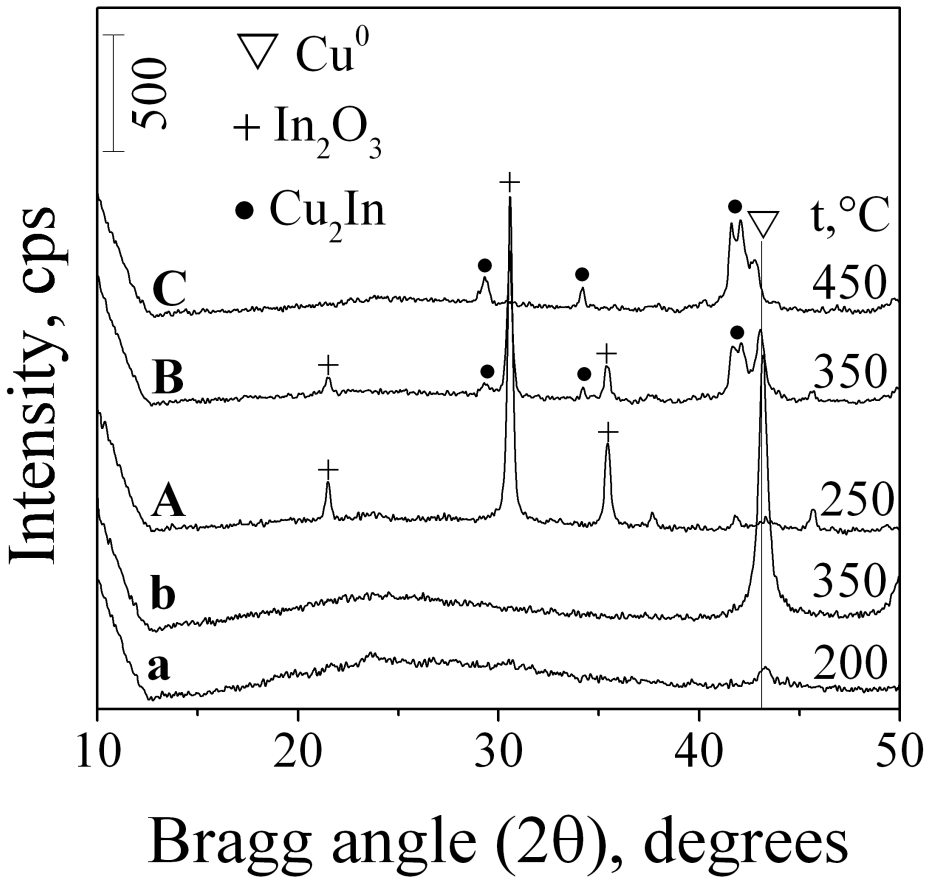

Figure 2. XRD patterns of 15CuX (a, b) and doped with 36 wt. % In_2O_3 (A, B, C) samples recorded at the indicated temperatures after 30 min treatment at each temperature in H_2 flow. The temperature was increased in 100 or 50 °C segments.

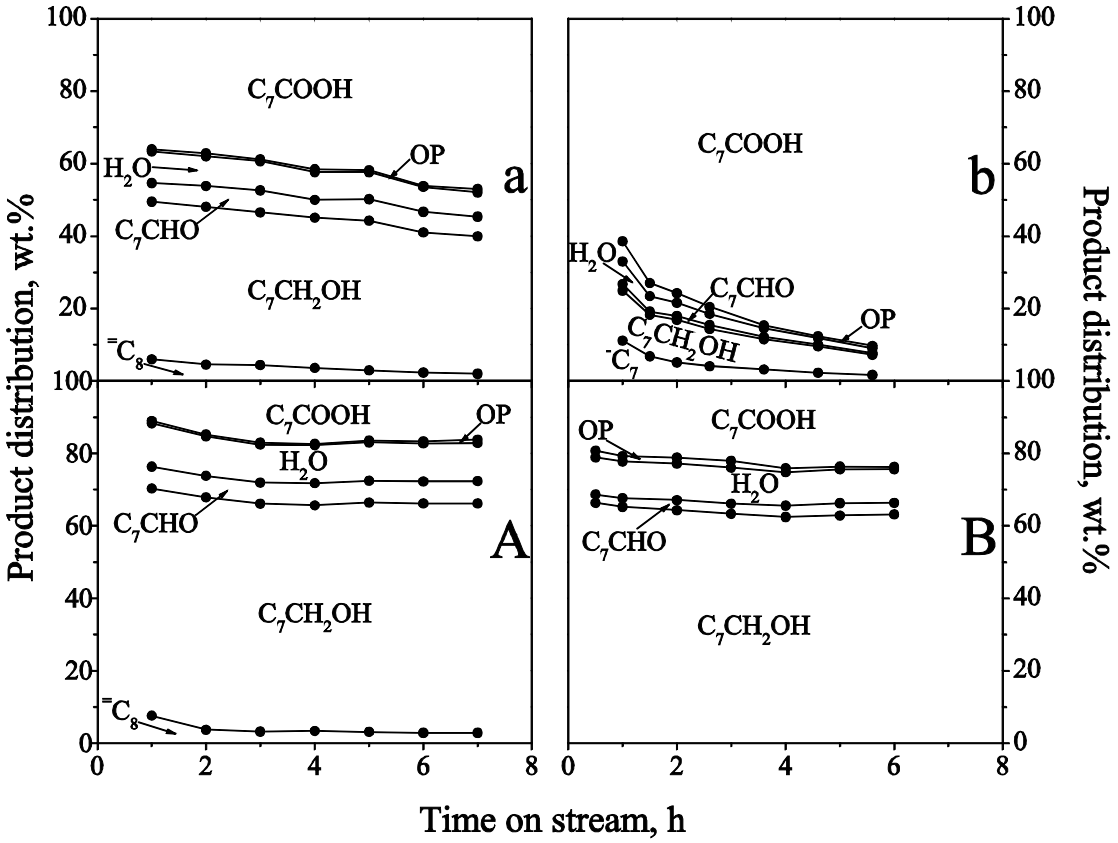

Figure 3. Octanoic acid hydroconversion over 16CuA (a) and doped with + 10 wt. % In_2O_3 (A) catalysts at 380 °C and over NiA (b) and doped with +10 wt. % In_2O_3 (B) catalysts at 300 °C are charactrized by distributions of main products as a function of time–on–stream at 21 bar total pressure. The WHSV of OA was 2.0 h^{-1}. Legends as in Fig.1. In addition: $^{-}C_7$ heptane.

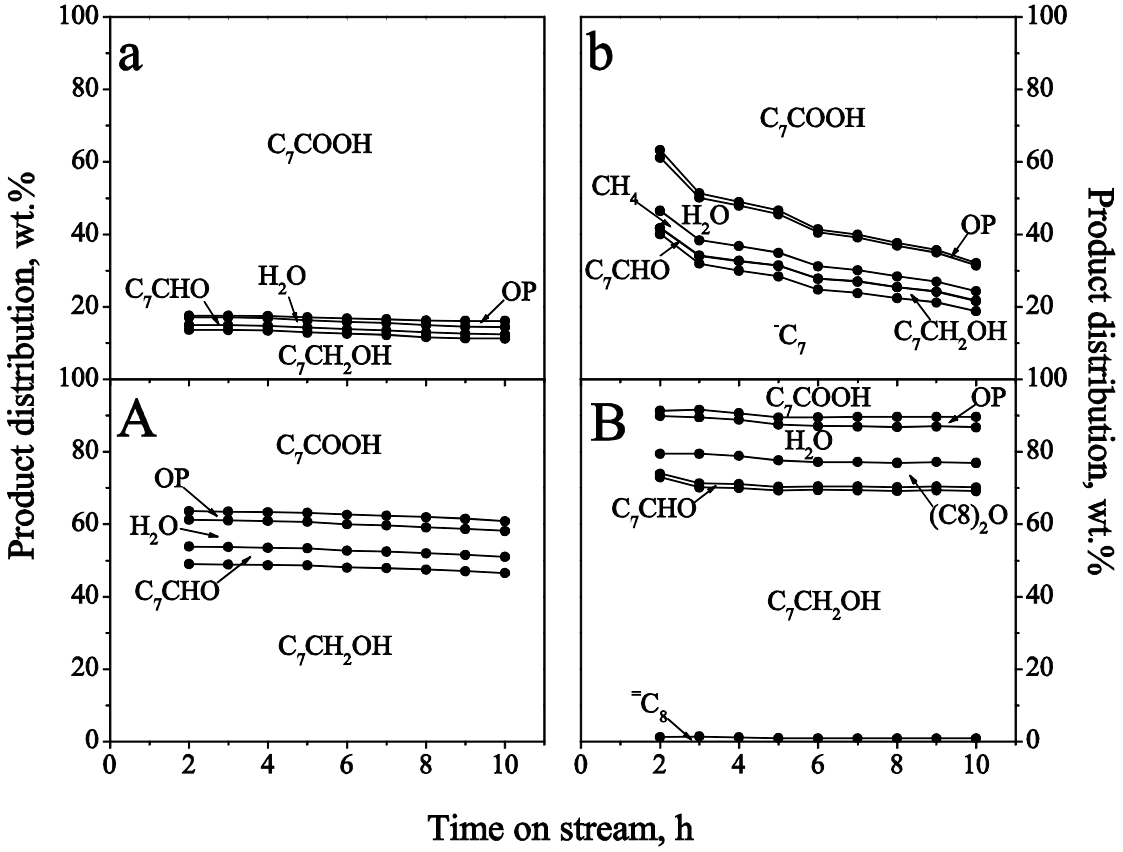

Figure 4. Octanoic acid hydroconversion over $9Cu/Al_2O_3$ (a), $9Cu/Al_2O_3$ + 10 wt. % In_2O_3 (A), $9Ni/Al_2O_3$ (b) and $9Ni/Al_2O_3$ + 10 wt. % In_2O_3 (B) are characterized by main products as a function of time–on–stream at 300 °C and 21 bar total pressure. The WHSV of OA was 2.0 h^{-1}. Legends as in Fig.1. In addition: $(C_8)_2O$ dioctyl ether.

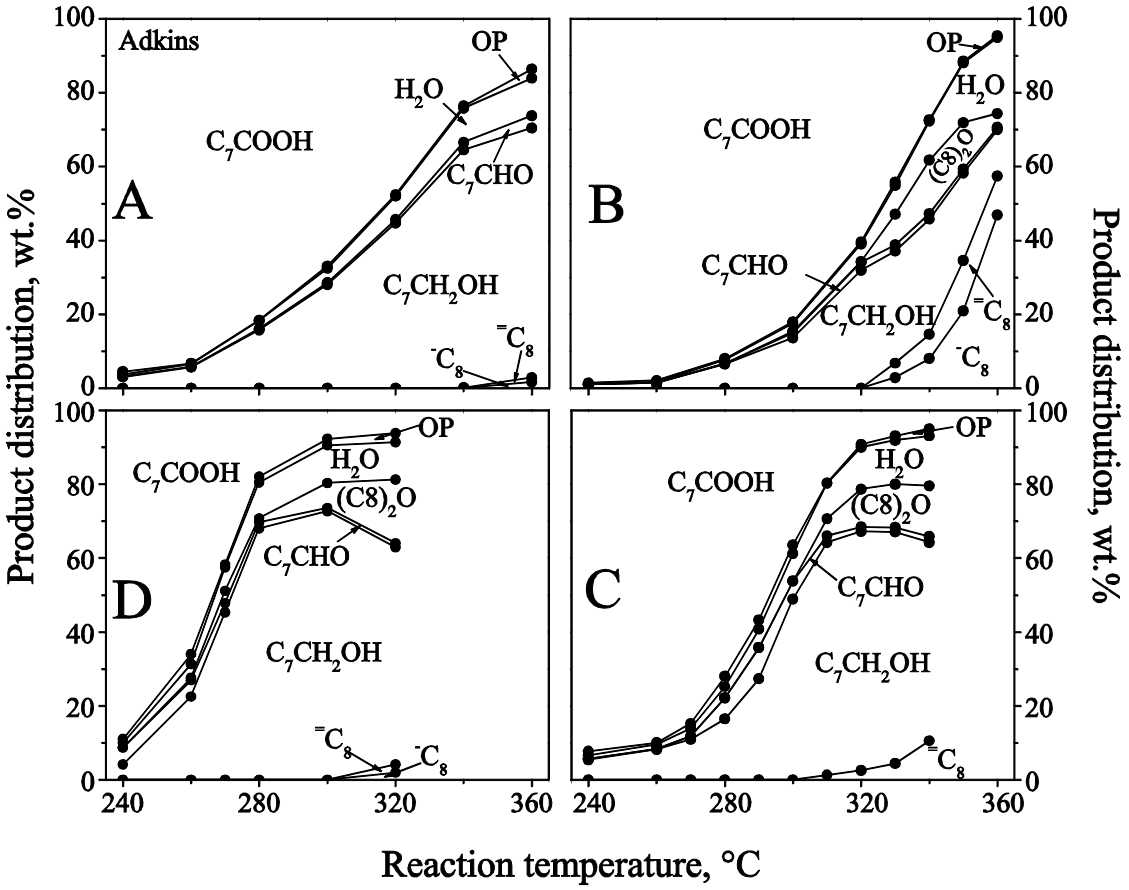

Figure 5. Octanoic acid hydroconversion over commercial Adkins (A), 9Cu/Al_2O_3 (B), 9Cu/Al_2O_3 + 10 wt. % In_2O_3 (C) and 9Ni/Al_2O_3 + 10 wt. % In_2O_3 (D) catalysts characterized by distributions of main products between 240 and 360 °C at 21 bar total pressure. The WHSV of OA was 2.0 h^{-1}. Legends as in Fig.1. In addition: $^{-}C_8$ octane, $(C_8)_2O$ dioctyl ether.

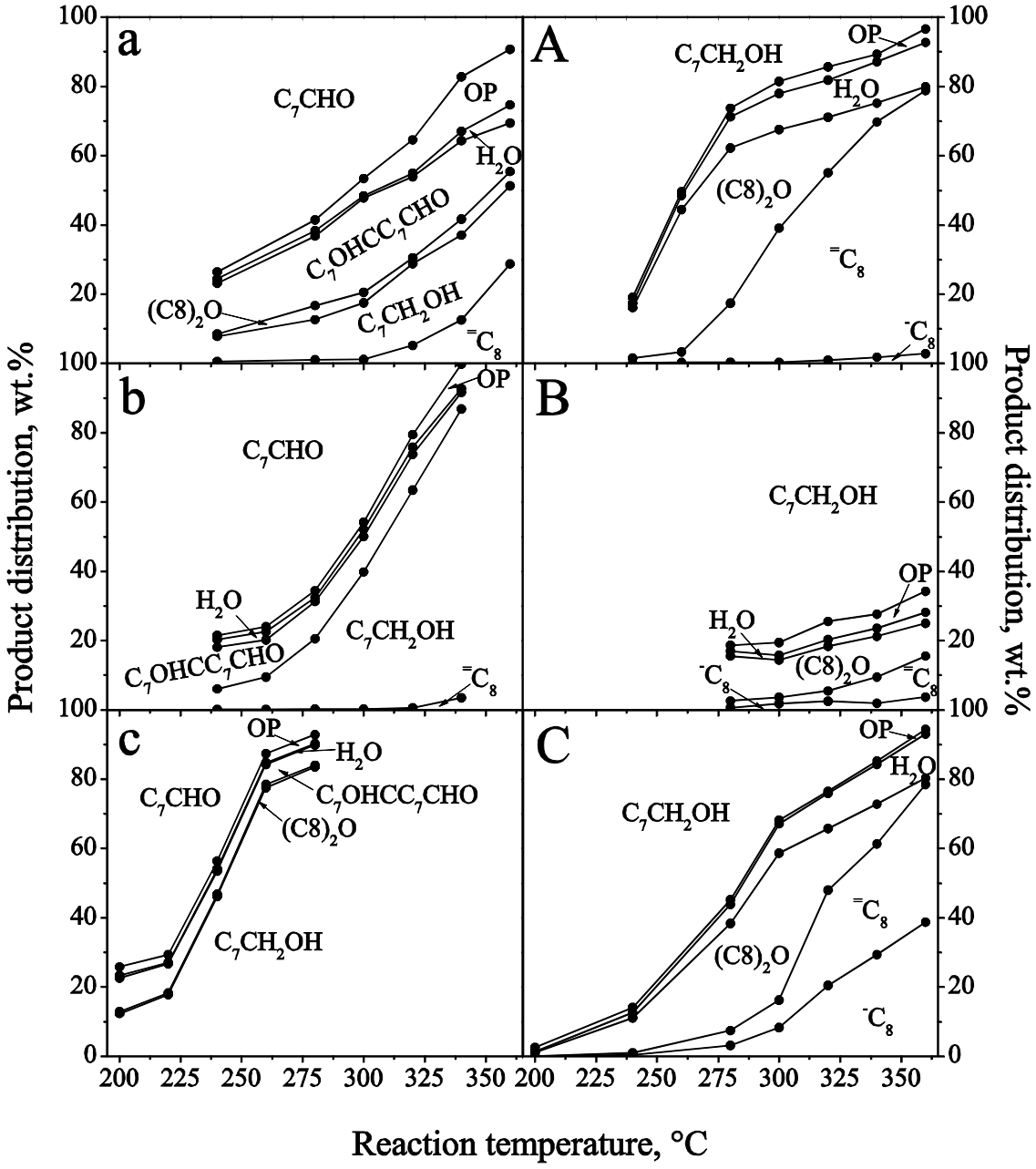

Figure 6. Octanal (a; b; c) and octanol (A; B; C) hydroconversion over Al_2O_3 (a; A), Al_2O_3 + 10 wt. % In_2O_3 (b; B) and 9Cu/Al_2O_3 + 10 wt. % In_2O_3 (c; C) catalysts characterized by distributions of main products between 200 and 360 °C at 21 bar total pressure. The WHSV of octanal and octanol was 2.0 h^{-1} similarly to octanoic acid reactant. Legends as in Fig.1. In addition: C_7OHCC_7CHO 2–hexyldec 2–enal (the product of octanal aldol condensation), $^{-}C_8$ octane, $(C_8)_2O$ dioctyl ether.

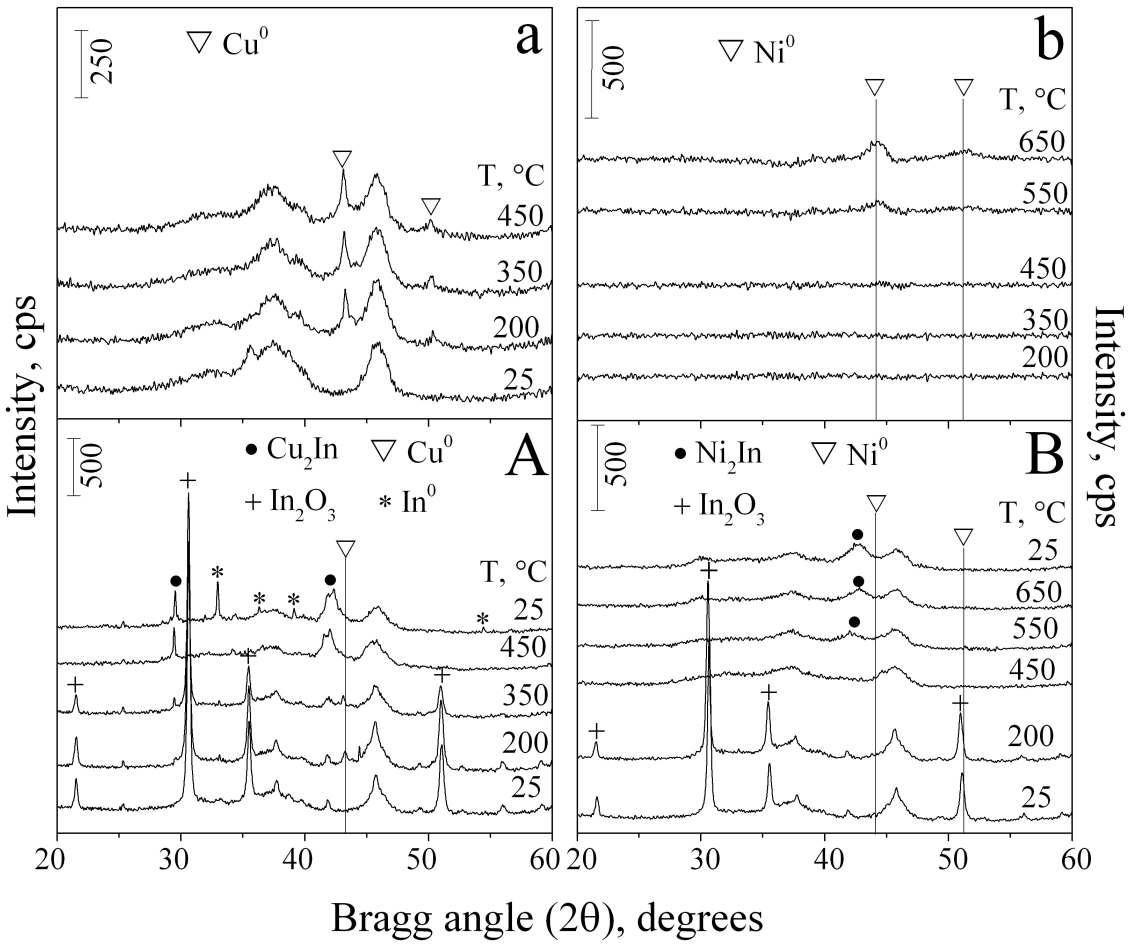

Figure 7. XRD patterns of $9Cu/Al_2O_3$ (a) and doped with 10 wt. % In_2O_3 (A), $9Ni/Al_2O_3$ (b) and doped with 10 wt. % In_2O_3 (B) catalysts. The diffractograms were recorded at the indicated temperatures after 30 min treatment at each temperature in H_2 flow. The temperature was increased in 100 or 50 °C segments.

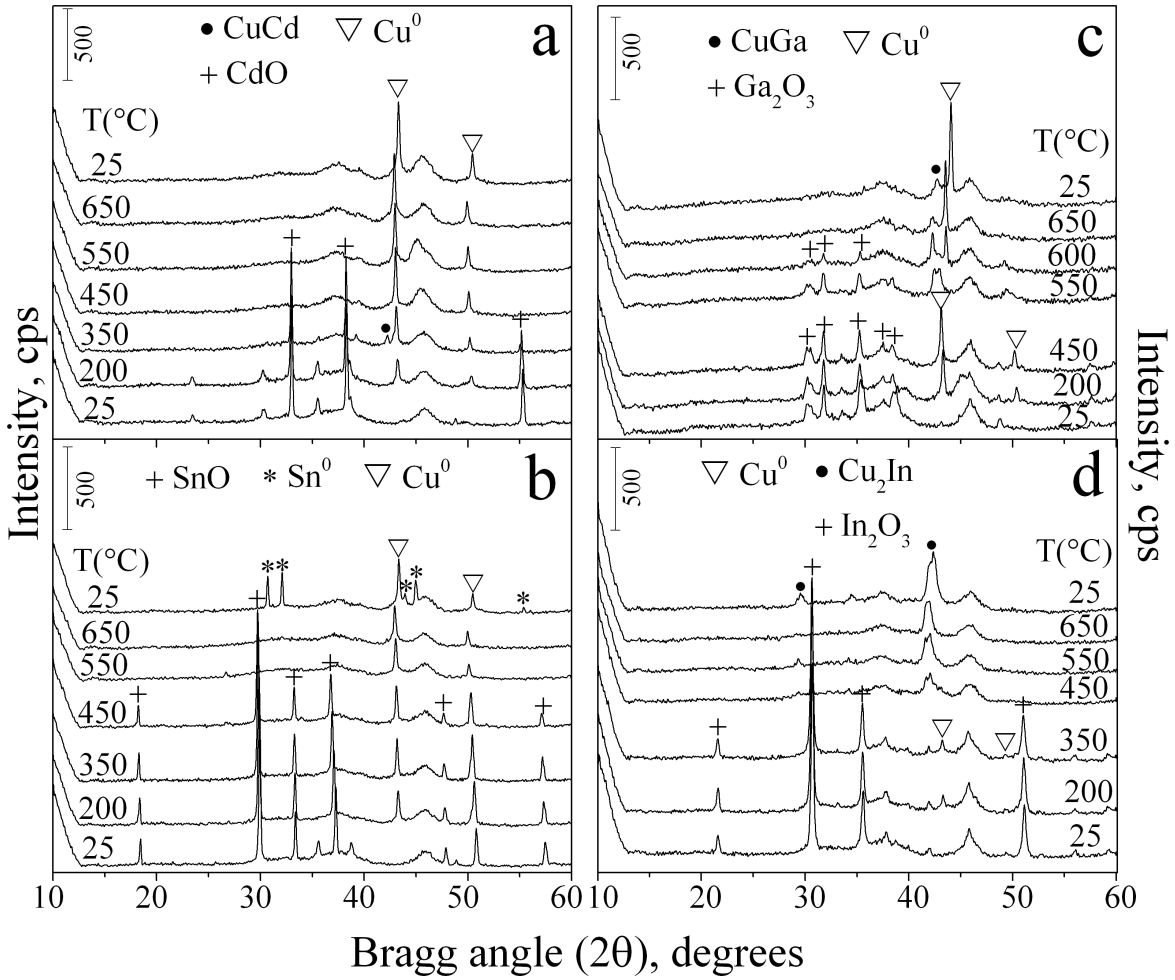

Figure 8. XRD patterns of $9Cu/Al_2O_3$ catalysts doped with 10 wt.% of CdO (a), SnO (b), Ga_2O_3 (c) and In_2O_3 (d). The diffractograms were recorded at the indicated temperatures after 30 min treatment at each temperature in H_2 flow. The temperature was increased stepwise by 100 or 50 °C.

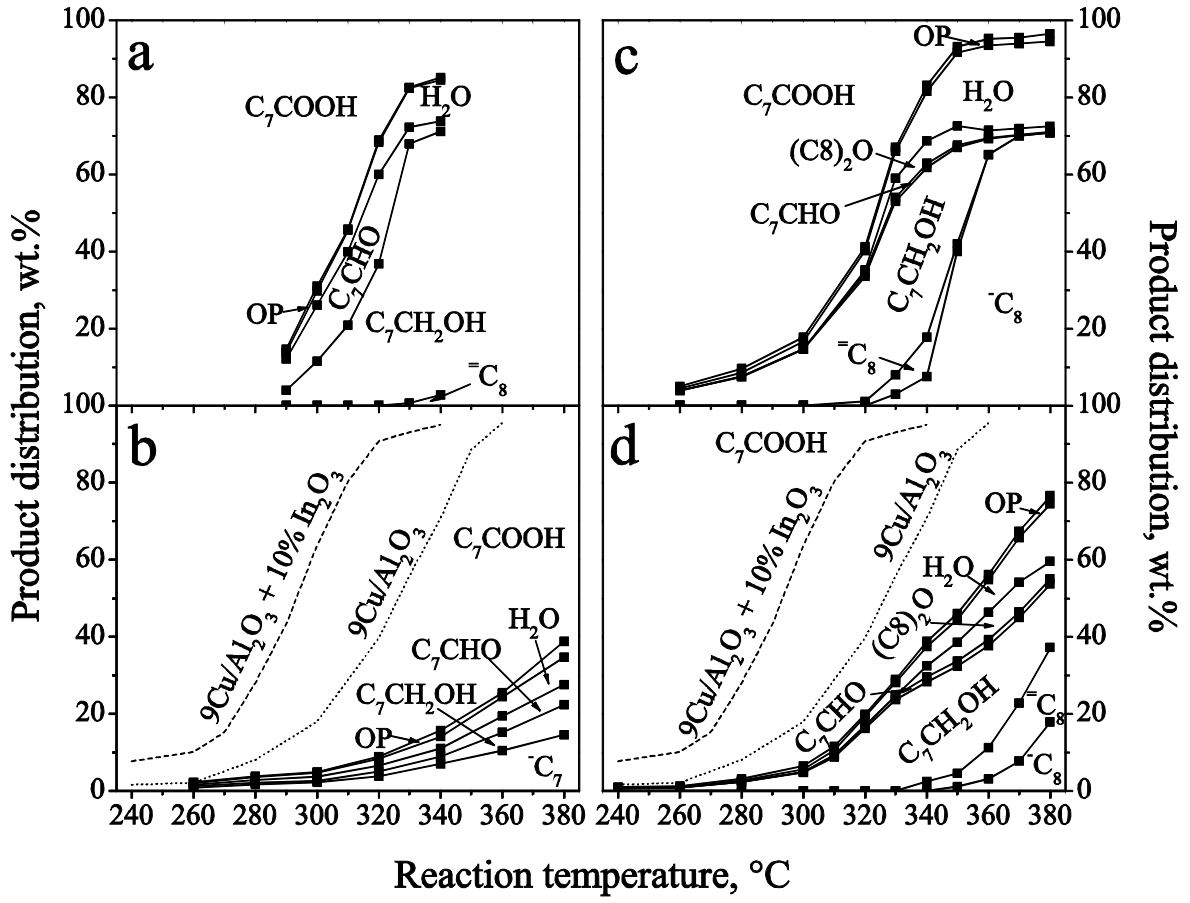

Figure 9. Octanoic acid hydroconversion over $9Cu/Al_2O_3$ + 10 % CdO pretreated at 350 °C (a), $9Cu/Al_2O_3$+ 10 % SnO pretreated at 450 °C (b), $9Cu/Al_2O_3$+ 10 % Ga_2O_3 pretreated at 450 °C (c) and 550 °C (d) catalysts characterized by distributions of the main products between 240 and 360 °C at 21 bar total pressure using stacked area graphs. WHSV of OA was 2.0 h^{-1}. Fig. 9b, d also shows the activity of $9Cu/Al_2O_3$ (dotted line) and $9Cu/Al_2O_3$ + 10 % In2O3 (dashed line) as a function of reaction temperature.

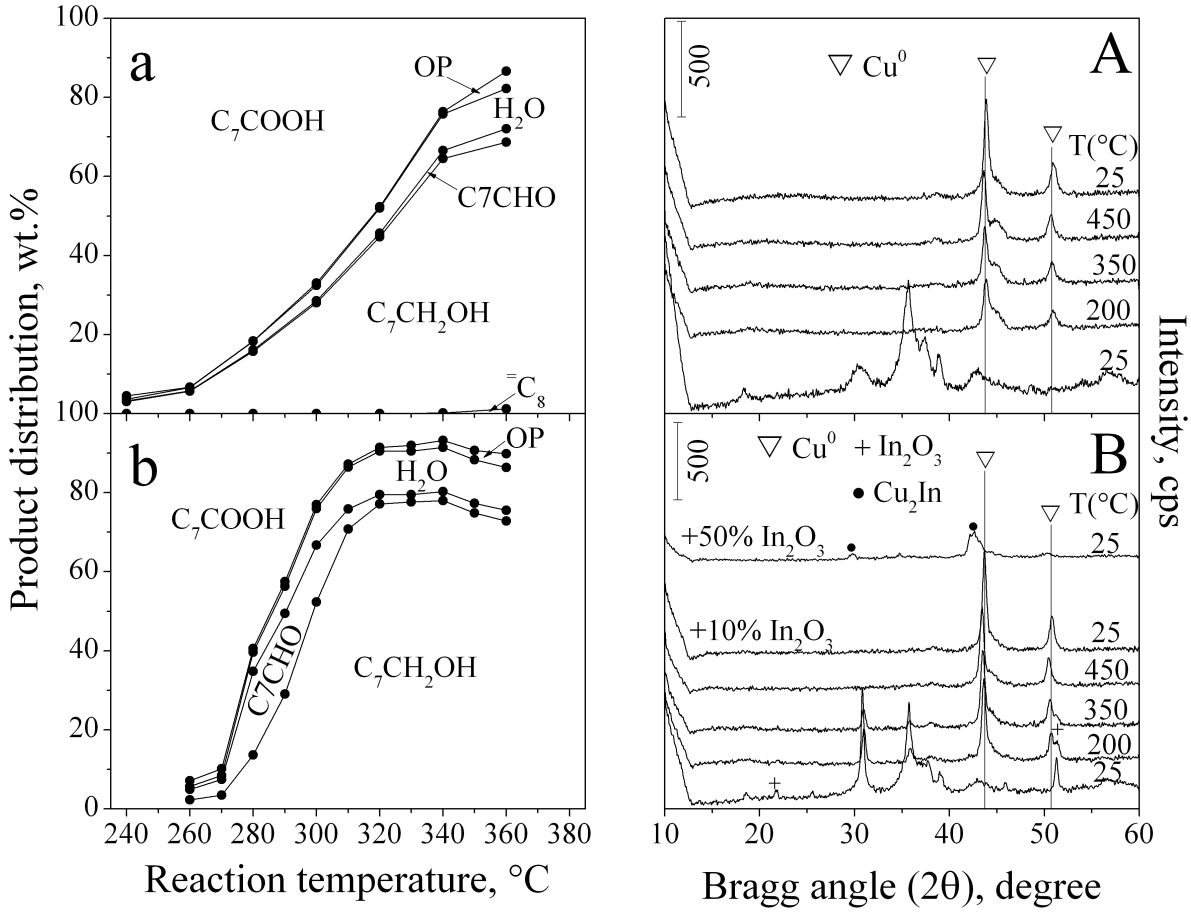

Figure 10. Octanoic acid hydroconversion over commercial Adkins catalysts without (a) and with 10 wt. % of co-catalyst (b) characterized by distributions of the main products between 240 and 360 °C at 21 bar total pressure using stacked area graphs. WHSV of OA was 2.0 h^{-1}. XRD patterns of commercial Adkins catalyst (A) and doped with 10 and 50 % In_2O_3 (B) samples recorded at the indicated temperatures after 30 min treatment at each temperature in H_2 flow. The temperature was increased in 100 or 50 °C segments.

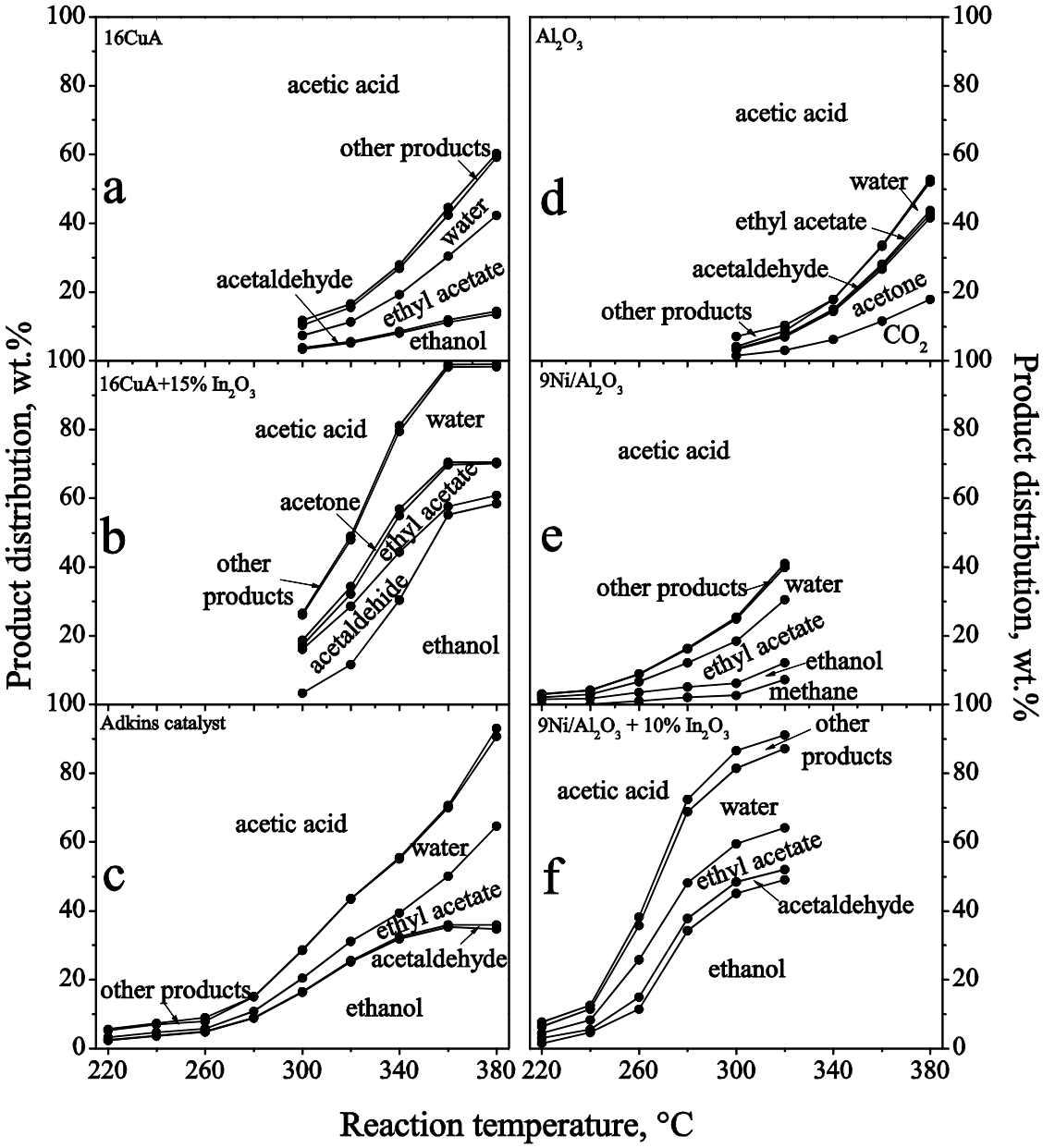

Figure 11. Acetic acid hydroconversion over 16CuA (a), 16CuA + 15 wt. % In_2O_3 (b), commercial Adkins (c), Al_2O_3 (d), 9Ni/Al_2O_3 (e) and 9Ni/Al_2O_3 + 10 wt. % In_2O_3 (f) catalysts characterized by distributions of the main products between 220 and 380 °C at 21 bar total pressure represented by stacked area graphs. WHSV of acetic acid was 1.0 h^{-1}.